1	Draft of Aug 27, 2020
2	Published as:
3 4 5	Wiedenbeck M, Trumbull RB, Rosner M, Boyce A, Fournelle JH, Franchi IA, Halama R, Harris C, Lacey JH, Marschall H, Meixner A, Pack A, Strandmann PAEP, Spicuzza MJ, Valley JW, Wilke FDH (2020) Tourmaline reference materials for the in situ analysis of
6 7 8	oxygen and lithium isotope ratio compositions. Geostand & Geoanal Res. 45: 97-119, doi: 10.1111/ggr.12362
9	Tourmaline reference materials for the <i>in situ</i> analysis of oxygen and
10	lithium isotope ratio compositions
11 12 13 14 15	Michael Wiedenbeck (1)*, Robert B. Trumbull (1), Martin Rosner (2) [†] , Adrian Boyce (3), John H. Fournelle (4), Ian A. Franchi (5), Ralf Halama (6) [‡] , Chris Harris (7), Jack H. Lacey (8), Horst Marschall (9) [§] , Anette Meixner (10), Andreas Pack (11), Philip A.E. Pogge von Strandmann (9) [⋄] , Michael J. Spicuzza (4), John W. Valley (4), Franziska D.H. Wilke (1)
17	(1) GFZ German Research Centre for Geosciences, 14473 Potsdam, Germany
18 19	 (2) Department of Marine Chemistry and Geochemistry, Woods Hole Oceanographic Institution, Woods Hole, MA 02543, USA
20	(3) Scottish Universities Environmental Research Centre, East Kilbride G75 0QF, UK
21	(4) Department of Geoscience, University of Wisconsin, Madison, WI 53706, USA
22	(5) School of Physical Sciences, Open University, Milton Keynes MK7 6AA, UK
23	(6) Department of Geology, University of Maryland, College Park, MD 20742, USA
24	(7) Department of Geological Sciences, University of Cape Town, Rondebosch 7701, South Africa
25	(8) National Environmental Isotope Facility, British Geological Survey, Keyworth NG12 5GG, UK
26	(9) Bristol Isotope Group, School of Earth Sciences, University of Bristol, Bristol BS8 1RJ, UK
27 28	(10) Faculty of Geosciences & MARUM - Center for Marine Environmental Sciences, University of Bremen, 28359 Bremen, Germany
29 30	(11) Geowissenschaftliches Zentrum, Universität Göttingen, 37077 Göttingen, Germany
31	† Current address: IsoAnalysis UG, 12489 Berlin, Germany
32	‡ Current address: School of Geography, Geology and Environment, Keele University, Keele ST5 5BG, UK
34	§ Current address: Institut für Geowissenschaften, Goethe-Universität, 60438 Frankfurt am Main, Germany
35 36 37	♦ Current address: Institute of Earth and Planetary Sciences, University College London and Birkbeck, University of London, London WC1E 6BS, UK
38 39	* Corresponding Author e-mail: michael.wiedenbeck@gfz-potsdam.de
40 41	Keywords: in-situ RM, homogeneity, $\delta^7 \text{Li}$, $\delta^{18} \text{O}$, $\delta^{17} \text{O}$, $\Delta^{17} \text{O}$
42 43 44	Three tourmaline reference materials sourced from the Harvard Mineralogical and Geological Museum and which are already widely used for the calibration of <i>in situ</i> boron isotope analyses are characterized here for their oxygen and lithium isotope compositions.

Homogeneity tests by secondary ion mass spectrometry (SIMS) showed that at sub-nanogram test portion masses their $^{18}\text{O}/^{16}\text{O}$ and $^{7}\text{Li}/^{6}\text{Li}$ isotope ratios are constant within \pm 0.27‰ and \pm 2.2‰ (1s), respectively. The lithium concentrations of the three materials vary over three orders of magnitude. SIMS homogeneity tests showed variations in ⁷Li/²⁸Si between 8% and 14% (1s), which provides a measure of the heterogeneity of the Li contents in these three materials. Here we provide recommended values for $\delta^{18}O$, $\Delta^{17}O$ and $\delta^{7}Li$ for the three Harvard tourmaline reference materials based on results from bulk mineral analyses from multiple, independent laboratories using laser- and stepwise fluorination gas mass spectrometry (for O), and solution multi-collector inductively-coupled plasma mass spectroscopy (for Li). These bulk data also allow us to assess the degree of inter-laboratory data that might be present in such datasets. This work also re-evaluates the major-element chemical composition of the materials by electron-microprobe analysis and investigates the presence of a chemical matrix effect on SIMS instrumental mass fractionation with regards to δ^{18} O determinations, which was found to be < 1.6% between these three materials. The final table presented here provides a summary of the isotope ratio values that we have determined for these three materials. Depending on their starting mass either 128 or 256 splits have been produced of each material, assuring their availability for many years into the future.

Key Words: tourmaline, lithium isotopes, oxygen isotopes, reference materials, SIMS, matrix effect

In situ analysis of boron isotope ratios in tourmaline by SIMS and LA-ICP-MS has become a widely used method for investigating fluid-rock interaction in igneous, metamorphic and hydrothermal systems, with important applications to ore genesis studies. Some of this work has been summarized in reviews by Slack and Trumbull (2011), Marschall and Jiang (2011) and in various chapters of the monograph by Marschall and Foster (2018). The rapid growth of B-isotope studies on tourmaline is partly due to the availability of well-characterized and demonstrably homogeneous tourmaline reference materials (RMs). Other stable-isotope systems that can be applied to tourmaline include H, Li and O, and these have shown their utility in several studies that employed bulk analysis of mineral separates (e.g., Taylor et al. 1999, Matthews et al. 2003, Siegel et al. 2016). However, the lack of characterized RMs that are known to be homogeneous at the nanogram to picogram sampling scale has prevented the application of in-situ methods to these isotope systems. This is unfortunate, as the combination of two or more isotope systems can reduce ambiguities in models built on laboratory data. In this study we provide O- and Li-isotope ratio data for three tourmaline RMs so as to partially meet this need.

Oxygen has three stable isotopes: ¹⁶O, ¹⁷O, and ¹⁸O, which have natural abundances of *ca.* 99.76%, 0.04% and 0.2%, respectively. By convention, the two isotope ratios of oxygen are expressed in delta-notation relative to Standard Mean Ocean Water (SMOW) as follows:

$$\delta^{18}O (\%) = [(^{18}O/^{16}O_{sample}/ ^{18}O/^{16}O_{SMOW}) - 1] * 1000$$
 eq. 1
$$\delta^{17}O (\%) = [(^{17}O/^{16}O_{sample}/ ^{17}O/^{16}O_{SMOW}) - 1] * 1000.$$
 eq. 2

where the absolute isotope abundance ratio for SMOW is set at $^{18}\text{O}/^{16}\text{O} = 0.00200520 \pm 0.00000045$ (Baertschi 1976) and $^{17}\text{O}/^{16}\text{O} = 0.0003799 \pm 0.0000008$ (Li *et al.* 1988). There is

abundant literature documenting the utility of oxygen isotopes in identifying fluid provenance, constraining fluid/rock interaction and for isotope exchange geothermometry (e.g., Valley and Cole 2001, Valley 2003, Sharp *et al.* 2016). For most fractionation processes, $\delta^{17}O$ shows a close correlation with $\delta^{18}O$. However, small, mass-dependent deviations from such a correlation can now be resolved in terrestrial samples (Barkan and Luz 2005, Pack and Herwartz, 2014). Such mass-dependent variations in $\delta^{17}O$ are a new tool in understanding oxygen isotope fractionation and/or reservoir-exchange processes (e.g., Herwartz *et al.* 2015, Sharp *et al.* 2016). Until now no certified values are available for any silicate or oxide calibration material for $\delta^{17}Ovsmow$, although recent efforts have been made to characterize San Carlos olivine and there are ongoing efforts to standardize the treatment of such data (e.g., Pack *et al.* 2016, Sharp *et al.* 2016, Miller et al. 2020, Wostbrock *et al.* 2020). Although the efforts presented here do not represent an attempt at an ISO-compliant certification, we nonetheless believe they are a valuable contribution towards addressing this shortage.

Lithium has two stable isotopes, 6 Li and 7 Li, with natural abundances of ca. 7.6% and 92.4%, respectively, though their abundance ratio varies considerably in nature. For example, a difference of some 30‰ exists between unaltered MORB and sea water (e.g., Tomascak 2004). The Li isotope system can undergo large fractionation between geological materials (fluids, minerals, melts) during processes including fluid-rock interaction, fluid or melt unmixing, (re)crystallization and diffusion, making it valuable for many geologic applications (e.g., Teng $et\ al$. 2004, Tomascak $et\ al$. 2016). Li isotope ratios are typically reported in δ -units with reference to lithium carbonate, L-SVEC (now NIST SRM-8545; Flesch $et\ al$. 1973, Brand $et\ al$. 2014) as follows:

$$\delta^7 \text{Li }(\%_0) = \left[(^7 \text{Li}/^6 \text{Li}_{\text{sample}} / ^7 \text{Li}/^6 \text{Li}_{\text{L-SVEC}}) - 1 \right] * 1000$$
 eq. 3

where the absolute isotopic abundance ratio for L-SVEC is set at $^6\text{Li}/^7\text{Li} = 0.08215 \pm 0.00023$ (combined uncertainty at coverage factor k = 2; Coplen 2011, Harms and Assonov 2018), equivalent to $^7\text{Li}/^6\text{Li} \approx 12.173$.

Both oxygen and lithium isotope ratios in tourmaline can readily be determined by SIMS on polished sample surfaces with a spatial resolution of < 20 μ m and analytical repeatabilities at or below \pm 1‰ (1s) in the case of $\delta^7 \text{Li}$ and better than \pm 0.2‰ (1s) in the case of $\delta^{18} \text{O}$. However, in practice such measurements are rarely made due to a lack of suitable tourmaline RMs. For this study we turned to the widely-used Harvard tourmaline suite. Dyar *et al.* (2001) reported values of $\delta^{18} \text{O}$ for the tourmaline RMs elbaite, schorl and dravite studied here, albeit prior to the sample splitting done as part of the current investigation. Those analyses were done in one laboratory (Southern Methodist University) only and no isotope homogeneity tests for O isotopes were carried out at test portion masses relevant for microanalytical applications. Lin *et al.* (2019) reported values of the Li isotope composition of the Harvard schorl and elbaite materials based on solution-nebulisation ICP-MS. Likewise, no isotope homogeneity tests were reported in that study. Finally, Dyar *et al.* (2001) also reported a single set of δD values for all three of the materials that are the focus of this current study (see below).

A particular concern in the determination of isotope amount ratios of light elements in tourmaline and other minerals where a wide major element compositional range exists is the possible presence of a chemical matrix effect. Bell (2009) discussed the chemical matrix effect in the context of SIMS Li isotope analyses in olivine. Because multiple and chemically diverse tourmaline RMs exist for B-isotope analysis, workers have been able to demonstrate a small but significant chemical matrix effect in both SIMS (e.g., Kutzschbach *et al.* 2017, Marger *et al.* 2020) and ICP-MS applications (Míková *et al.* 2014). The issue of a matrix effect for the lithium and oxygen isotope SIMS analyses is discussed below.

Materials

Dyar *et al.* (2001) and Leeman and Tonarini (2001) reported on the major-element compositions and chemical homogeneity of three megacrystic tourmaline samples from the Harvard Mineralogical and Geological Museum, designated elbaite, schorl and dravite (note: "dravite" is a misnomer, see below). Tonarini *et al.* (2003) and Gonfiantini *et al.* (2003) suggested a fourth natural tourmaline (IAEA-B4), which has a major element composition similar to that of the Harvard schorl, as a further RM for *in situ* chemical and B isotope analyses. We did not have access to large amounts of the B4 material with which to generate metrological splits, so we have not included this material in the current characterization project. Hence, this study focussed exclusively on the three materials described below:

<u>Elbaite</u> (Harvard Mineralogical and Geological Museum #98144): This sample is from a 17.5 g single crystal collected from a granitic pegmatite in Minas Gerais, Brazil.

<u>Schorl</u> (HMGM #112566): This sample is from a 48.4 g single crystal collected from a granitic pegmatite in Zambezia Province, Mozambique (Hutchinson and Claus 1956).

<u>Dravite</u> (HMGM #108796): This sample has been previously described as a 16.6 g single crystal collected from alluvium in Madagascar (Dyar *et al.* 2001), but this mass seems to be erroneous. Based on its size (Frondel *et al.* 1966, gives 560 grams as the mass) and locality, the sample was possibly derived from a granitic pegmatite. Of the amount of material provided to the first author by the Harvard Museum, two large, euhedral crystals with masses of 134 g and 194 g remain after producing our metrological splits (see below).

Based on the chemical analyses reported in Dyar *et al.* (2001) and in this study the schorl and elbaite samples are appropriately named, whereas the "dravite" term is misleading since this tourmaline has low Al-contents, high Ca and an Fe/(Fe+Mg) ratio of ~0.5, whereby Fe³⁺ dominates and substitutes for Al (Frondel *et al.* 1966). Using the current nomenclature of Henry *et al.* (2011) this composition is an intermediate schorl-dravite-feruvite, but in the interests of historical consistency we will continue to refer to the HMGM #108796 material as "dravite". The chemical classifications of the three materials are shown in Figure 1. We note that the δD (Dyar *et al.* 2001) and $\delta^{11}B$ (Leeman and Tonarini 2001) have already been reported for these materials (see Table 7). More recently, Marger *et al.* (2020) have reported revised $\delta^{11}B$ bulk values for the three tourmaline materials (also shown on Table 7) that are as much as 1.6% lower than the values published previously.

We used a riffle splitter in order to generate ~ 100 mg units of < 2 mm fragments from single crystals from each of the three tourmaline specimens; these were placed in 0.5 ml

screw-top plastic vials. In total we generated 256 vials of the elbaite, 128 vials of the schorl, and 512 vials of the dravite. In order to give these unique metrological identifiers, each set of splits has been given a Harvard catalogue number that is appended with an additional decimal place (i.e., 98144.1 Elbaite, 112566.1 Schorl and 108796.1 Dravite). With the exception of the wet chemical δ^7 Li data, which were performed on fragments removed from the parent samples prior to splitting, all data reported here were made on tourmaline fragments taken from such vials of the split material.

185 186 187

179

180

181 182

183

184

Homogeneity Assessments

188

Electron probe microanalysis (EPMA) for major elements

189 190 191

192

193

194

195

196

197

198

199

200

201

202

203

204

205

206

207

208

209

210

211

212

213

214215

216

217

218219

220

221

222

The characterization study by Dyar et al. (2001) reported homogeneity testing in the form of EPMA traverses across single sections of the original crystals as well as mean values from four independent EPMA laboratories. Most of those reported EPMA analyses, however, showed very low analytical totals, which can be improved upon by utilizing up-to-date EPMA procedures for optimal matrix correction accuracy. Also, there have been no data previously reported describing the chemical heterogeneity between random fragments that are more representative of each of the three materials. For this reason we conducted new EPMA analyses using a JEOL JXA8500F instrument at the GFZ Potsdam and a CAMECA SXFive FE instrument at the University of Wisconsin-Madison, both of which used a single vial of each tourmaline material prepared by riffle splitting during the current investigation. Both laboratories analysed six randomly selected fragments from a single split of each of the three tourmaline materials, whereby each fragment was analysed four times at broadly dispersed locations. In Madison, optically distinct (green vs. non-green) elbaite fragments were recognized and these were analysed separately (Table 1). Additional analyses at GFZ Potsdam were made of the silicate glass NIST 610 for an internal precision and repeatability check.

The EPMA analytical results and method descriptions are reported in Table 1 and the full data set is available in electronic supplement Table 1. Variations were found in the degree of homogeneity in these sets of fragments, making it difficult to define unique recommended values for the schorl and the dravite RMs. This is especially problematic for the elbaite RM, where the Madison EPMA results show distinct populations based on MgO, Al₂O₃ and FeO concentrations for grains separated by colour (a distinction not made in the Potsdam contribution). Notwithstanding the variable homogeneity of the tourmaline RMs, the EPMA results of the two laboratories are in good agreement with each other and, with the exception of B₂O₃, with the previously reported concentration values in Dyar et al. (2001). The new EPMA results for B₂O₃ agree well with the values reported for non-EPMA techniques by Dyar et al. (2001). Thus, for schorl, the EPMA B2O3 "grand mean" values from Potsdam $(10.1 \text{ m}/100\text{m} \pm 0.4, 1\text{s})$ and Madison $(9.6 \text{ m}/100\text{m} \pm 0.7, 1\text{s})$ are consistent with the non-EPMA range of 9.7 to 10.3 m/100m; for dravite the EPMA results are 10.1 m/100m \pm 0.5 (1s) for Potsdam and 9.9 m/100m \pm 0.5 (1s) for Madison, compared with the non-EPMA range of 10.0 to 10.3 m/100m reported by Dyar et al. (2001). The inter-grain variability of the elbaite RM is relatively high for Fe, Mg and Al, but the variations for boron are no larger in elbaite

than in the other two tourmaline RMs (Table 1). Furthermore, the elbaite EPMA values from both laboratories are in good agreement with those of non-EPMA techniques from Dyar *et al.* (2001). The elbaite B_2O_3 "grand mean" value for Potsdam is 10.6 ± 0.5 m/100m (1s), for Madison "non-green" and "green" populations the values are 10.1 ± 0.8 m/100m and 10.0 ± 0.5 m/100m, respectively; the range from non-EPMA techniques (Dyar *et al.* 2001 Table 4) is 10.1 to 10.2 m/100m.

We conclude that schorl 112566.1, dravite 108796.1 and to a certain extent elbaite 98144.1 are suitable for use as EPMA calibration and quality control materials. Any particular fragment composition should fall within the bounds of the reported compositions in Table 1, provided at least 98 m/100m of the composition (including Li, OH etc.) is accounted for in the EPMA matrix correction.

233234235

229

230231

232

SIMS Lithium Testing

236237

238

239

240241

242

243

We used the Potsdam Cameca 1280-HR instrument to assess both the Li concentration and δ^7 Li heterogeneities in the three tourmaline materials. For this purpose a mount was made that contained multiple fragments from each of the three tourmaline splits as well as a mm-sized piece of the NIST 610 silicate glass. An additional benefit of the concentration test is that these data contribute towards refining the absolute Li concentrations reported by Dyar *et al.* (2001), which showed large discrepancies between analytical methods. However, we specifically note that we do not contribute any further absolute concentration data to this discussion.

244245246

247

248249

250

251

252

253

254255

256

257

258

259

260

261262

263

264

265266

267

Lithium concentration evaluation

Our SIMS analyses used a \sim 25 pA $^{16}O^{-}$ primary beam focussed to a \sim 2 µm diameter spot with a total impact energy of 23 keV. Data were collected using a 10 µm raster, thereby assuring a flat-bottom crater geometry. Each analysis was preceded by a 170 s pre-sputtering using a 2 nA primary beam and a 20 μm raster in order to locally remove the conductive gold coat and to suppress any surface contamination; actual data collection used a 10 µm raster, which was compensated with the instrument's dynamic transfer option. Prior to data collection we completed automatic centring routines on the field aperture in X and Y. The mass spectrometer was operated at a mass resolution of $M/\Delta M \approx 3700$, which is more than adequate to resolve both the ⁶Li¹H⁺ ion from ⁷Li⁺ and the ²⁷Al¹H⁺ ion from the ²⁸Si⁺ mass station. A 2000 * 2000 µm square field aperture, equivalent to a 20 * 20 µm field-of-view, and a 150 µm contrast aperture were used. The energy window was set to a 40 eV width and no offset voltage was applied. Data were collected using a 40 µm wide entrance slit and a 280 µm wide exit slit running in mono-collection mode using the ETP pulse counting system, to which a synthetic 46.2 ns deadtime was applied using a delay circuit in our preamplifier. A single analysis consisted of 20 cycles of the peak stepping sequence ⁷Li⁺ (2s), ²⁸Si⁺ (2s). A single analysis, including pre-sputtering, auto-centring and data acquisition, required 7 minutes. We conducted 116 such analyses over the course of one automated analysis sequence. Using these analytical conditions we had a typical ²⁸Si⁺ count rate of around 50,000 ions per second. The total amount of material removed during data acquisition was very small; our best estimate of the volume of the sputter crater, based on white light profilometry, is $\sim 3.2 \, \mu \text{m}^3$, equivalent to a test portion mass of $\sim 10 \, \text{pg}$. The dataset from this experiment,

along with the Li concentrations based on the calibration using the NIST 610 glass, are shown in electronic supplement Table 2. The equivalent Li₂O mass fractions in m/100m, along with other determinations from Dyar *et al.* (2001), are also given in Table 2. We explicitly note that the Li mass fractions reported here are not robust as the NIST 610 silicate glass is, at best, a poor matrix match for the tourmalines we investigated.

Lithium isotope evaluation

Because Li concentration varies by a factor of 1000 between the elbaite and dravite materials (Table 2) it was not possible to run all three SIMS δ^7 Li homogeneity experiments under identical conditions. To accommodate such large differences in mass fractions we modified the 16 O- primary current, the ion detection system and the total count times, with the goal of achieving better than \pm 0.2-‰ (1s) internal uncertainties on the individual analyses. Hence, the test portion masses, as determined by white light profilometry, also varied between materials. A summary of the specific analytical conditions is included in Table 3.

A common feature of all three sets of ⁷Li⁺/⁶Li⁺ SIMS data is that the primary beam was operated in Gaussian mode with a total impact energy of 23 keV. Tests using a Köhler mode primary beam showed poor repeatability, and we therefore abandoned this approach. Pre-sputtering employed either a 20 or 30 µm raster, which was reduced to a 15 x 15 µm raster during data collection. The dynamic transfer option of the instrument was used to actively compensate for this rastering. Automatic beam centring on the field aperture in both X and Y was conducted before each analysis. The mass spectrometer was operated with a 40 eV energy window, using no energy offset, in conjunction with a mass resolving power $M/\Delta M > 1900$. Data were recorded in multi-collection mode employing an NMR field control system. Ions were collected using the L2 and H2 trollies for ⁶Li⁺ and ⁷Li⁺, respectively; the actual detectors used varied between the experiments depending on Li concentration in the tourmaline RMs (see Table 3); for those experiments using electron multipliers we did an automatic voltage scan prior to each analysis so as to minimize drift due to aging of the first dynode. Analytical points were dispersed over multiple fragments in the epoxy mount and additionally, several points were placed closely together on a single fragment of the same tourmaline material as a "drift monitor" (DM) in order to test for a time dependent drift in the ion detection system. After setting all points, the analysis sequence of all non-DM points was randomized. Making the reasonable assumption that the RMs are homogeneous in isotopic composition within a confined area of a few hundred micrometres, the results of "drift monitor" determinations can also be used to quantify the repeatability of the given analytical design. The results from the lithium isotope ratio homogeneity tests of the three tourmaline materials are shown in Table 3, and the full set of results are available from electronic supplement Table 3.

The Li homogeneity assessment on the schorl material presented a special case in two respects. Firstly, the Li concentration in schorl is similar to that of the NIST 610 silicate glass (Table 2). We therefore conducted interspersed $^7\text{Li}^+/^6\text{Li}^+$ determinations on this glass as a comparison test for the repeatability, whereby we assume that the NIST 610 synthetic glass is homogeneous over the few hundred micrometres used for this assessment. Secondly, the schorl material was particularly challenging from the perspective of the ion count rates that it provided. Under the requirement that the $^{16}\text{O}^-$ primary beam current was in the range between 20 nA and 0.5 nA, it was found that one of the Li isotopes inevitably provided a count rate in

the gap between optimum performance of our FC using a e11 Ω resistor and the Hamamatsu pulse counting system (this "gap" is roughly between 2e6 and 2e5 counts per second). Ultimately, we elected to use a compromise where the $^7\text{Li}^+$ signal was towards the low end of the optimal range for our FC amplifier (3.9e6 cps) and the $^6\text{Li}^+$ signal was slightly above the optimal range for our pulse counting system (3e5 cps). An automatic voltage scan conducted on the Hamamatsu electron multiplier prior to each analysis was able to compensate the drift in the detector at the 0.5‰ level over the six hours run duration. We have not investigated how large this drift would have been without applying the detector voltage correction.

320321322

313

314

315

316

317

318319

SIMS Oxygen Testing

323324

325

326

327

328

329

330

331

332

333

334

335

336

337

338

339

340

341

342

343

344

345

346

347

348

349

350351

352

We assessed the $\delta^{18}O$ heterogeneity of the three tournaline materials with the Potsdam Cameca 1280-HR instrument. These analyses employed ¹³³Cs⁺ primary ion beam with a total impact energy of 20 keV and ~2.5 nA beam current focused to a ca. 5 µm diameter spot on the polished sample surface. Each analysis was preceded by a 2.5 nA, 60 s pre-sputtering in conjunction with a 20 um raster. All analysis points were within 8 mm of the centre of the sample mount. Negative secondary ions were extracted using a -10 kV potential applied to the sample holder, with no offset voltage applied, in conjunction with a 40 eV wide energy window, which was mechanically centred at the beginning of the analytical session. Normal incidence, low energy electron flooding was used to suppress sample charging. Each analysis was preceded by an automatic centring routine for the instrument's field aperture in both X and Y and the centring of the beam on the contrast aperture in the Y direction only. A square 5000 * 5000 μm filed aperture, equivalent to a 50 * 50 μm field-of-view, a 400 μm contrast aperture, and a 114 um wide entrance slit and a 500 um wide exit slits were used for this fully automated data collection sequence. The instrument was operated in multi-collection Faraday cup mode using the instrument's NMR field stabilization circuitry. The ion count rate on the ¹⁶O peak was typically 2*10⁹ cps. Each analysis consisted of 20 integrations of 4 seconds each. Data were collected using a 10 x 10 µm primary beam raster, thereby assuring a flat bottom crater, for which the dynamic beam transfer option of the secondary ion optics was used to compensate. The analytical stability was monitored by interspersed measurements of the NIST 610 silicate glass that was embedded in the same 1-inch diameter sample mount. Using this approach we detected an analytical drift amounting to 0.013% per hour over the course of the 16.6 hours of continuous data acquisition. The analytical repeatability for the n = 29 determinations on the NIST 610 glass drift monitor was \pm 0.33% (1s), which improved to \pm 0.21% after applying a linear drift correction (Table 4, electronic supplement Table 4). The analytical repeatability on all three of the Harvard tourmalines was similar to this value (Table 4), and hence we conclude that no major oxygen isotope heterogeneity is present in any of the three tourmaline RMs. The volume of a single crater that was produced under these conditions was determined to be 115 µm³ using white light profilometry, including the presputtering and beam centring processes, equivalent to a test portion mass of ~350 pg (based on a density of $\rho = 3.0 \text{ g/cm}^3$ for tourmaline).

353354

Bulk Sample Isotope Determinations

Solution MC-ICP-MS analysis of δ⁷Li

Lithium isotope compositions were determined on acid-digested sample solutions by MC-ICP-MS in four laboratories: Woods Hole Oceanographic Institution, the University of Maryland, the University of Bristol, and the University of Bremen. The only information exchanged between the laboratories prior to analysis concerned the approximate Li concentrations in the tourmalines and the need for a prolonged, high-pressure dissolution in order to achieve complete digestion. Each laboratory performed one or two independent dissolutions of separate aliquots of each RM, and in all but a few cases the separate dissolution samples were analysed between 2 and 5 times each. The analytical technique descriptions for each of the participating labs are given below, a summary of the results along with the final recommended values are shown in Table 5 and a compilation of all the data are given in electronic supplement Table 5. We note that the Li isotope analyses of elbaite #98144 at the University of Bristol were previously published by Ludwig *et al.* (2011). Independent of our study, Lin *et al.* (2019) reported Li isotope values for the Harvard schorl #112566 and elbaite #98144 analysed by solution ICP-MS. Their results are also shown on Table 5.

372373374

375

376

377

378

379

380 381

382

383

384

385

386387

388

389

390

391

357

358359

360361

362

363

364365

366367

368

369

370

371

Woods Hole Oceanographic Institution:

Multiple tourmaline fragments with a total mass between 1 and 10 mg were crushed and then digested in steel-clad Teflon bombs under pressure at 120°C in a mixture of 1.5 ml HF and 0.5 ml concentrated HNO₃ for 2 days. The dried samples were taken up in 9 ml 1N HNO₃ with 80% methyl alcohol from which the Li fraction was separated by ion chromatography using a 10 ml AG 50W X8 (200-400 mesh) column (see Tomascak et al. 1999). The Li cuts were analysed with a Thermo-Finnigan NEPTUNE MC-ICP mass spectrometer using sample/calibrator bracketing with NIST 8545 (see Rosner et al. 2007). The total Li blank of this procedure was < 0.5 ng, which is negligible for the elbaite and schorl materials and less than 1% of the Li recovered from an analysis of the dravite material. Since the isotopic composition of the blank can be assumed to be in the natural terrestrial range, we conclude that a 1% Li contribution from the blank does not significantly impact the determined δ^7 Li values. The internal precision of each ⁷Li/⁶Li measurement was < 0.1‰ (2SE). Multiple analysis of sample solutions for schorl and elbaite gave repeatabilities < 0.4% (2s, n = 4); the dravite solutions were measured only once. The δ^7 Li values from individual solution aliquots (schorl and dravite) deviated by less than 0.8% (Table 5). Rosner et al. (2007) estimated the trueness of the δ^7 Li values from this procedure at ca. 0.5% or better based on concurrent analyses of independent RMs - NASS-5 from the North Atlantic and IAPSO from the Mid-Atlantic, as well as four basaltic to andesitic rock RMs (BHVO-1, BCR-2, JA-1 and JB-2).

392393394

University of Maryland:

Tourmaline fragments having total masses ranging between 0.2 and 13.6 mg were lightly crushed and then cleaned for 15 minutes in an ultrasonic bath using Milli-Q water (18.2 M Ω /cm). Two separate dissolution aliquots were obtained using the following procedure. Sample digestion took place in steel clad Teflon bombs at 160°C under pressure in a 3:1 mixture of concentrated HF and concentrated HNO₃. The dried residua were refluxed with concentrated HNO₃, dried again and repeatedly refluxed with concentrated HCl until all fluorides were converted into chlorides and clear solutions were obtained. The final dried

residua were taken up in 1 ml 4M HCl, and the Li fraction was separated by ion chromatography in columns loaded with Bio-Rad AG 50w-x12 (200-400 mesh) using the procedure described by Rudnick et al. (2004). Lithium loss during column chemistry was monitored by taking an additional 2 ml cut after the Li cut from each column. The total loss during this study was between 0.6% and 1.3% of the total Li in the sample, which does not affect the Li isotopic composition significantly (Marks et al. 2007). Lithium isotope analyses were made on a Nu-Plasma MC-ICP-MS instrument (for details see Teng et al. 2004). Each analysis was bracketed by measurements of a standard solution of the Li-carbonate RM NIST 8545, and the ⁷Li/⁶Li value for the analysis was calculated relative to the average of the two bracketing runs. The total procedural blank during the course of the study was equivalent to a voltage of 4 mV for ⁷Li⁺ ions. This compares to a voltage of 1-1.5 V obtained for a solution with 50 μg/l Li at a 40 μl/min uptake rate, resulting in a sample/blank ratio of ~300. The internal precisions of ⁷Li/⁶Li measurements based on two blocks of 20 ratios each, was generally $\leq 0.2\%$ (2s). The repeatability of the method, based on > 100 analyses of a purified NIST 8545 standard solution, is $\leq 1.0\%$ (2s, see Teng et al. 2004). Analytical trueness was monitored during each session by multiple measurements of two reference solutions: seawater IRMM-016 (Qi et al. 1997) and an in-house UMD-1 quality control material (a purified Li solution from Alfa Aesar®). The results for both reference solutions agree within uncertainties with previously published values. Two measurements of the nepheline syenite RM STM-1 yielded +3.2 and +4.1%, which are within the range of previously published values (Halama et al. 2008). The long-term trueness of Li isotope analyses in the Maryland lab is monitored by multiple analyses of the BHVO-1 basalt RM, which gave $4.4\% \pm 0.7$ (1SE), which is in good agreement with published values (4.3 to 5.8%; James and Palmer 2000, Chan and Frey 2003, Bouman et al. 2004, Rudnick et al. 2004).

425426427

428

429

430

431

432

433

434

435

436 437

438

439

440

441

402 403

404

405

406

407

408

409

410 411

412

413

414

415

416

417418

419

420

421

422

423

424

University of Bristol:

The determinations on each of the three RMs were based on between 1 and 2 mg of material that was finely powdered, from which two separate aliquots were dissolved in the following three steps: first with a combined dissolution in a 2:6:1 ratio of concentrated HF-HNO₃-HClO₄ (where the perchloric acid is included to inhibit the formation of insoluble Lifluorides, see Ryan and Langmuir 1987), followed by concentrated HNO₃ and then 6M HCl. The dissolution process incorporated repeated ultra-sonication. The dissolved samples were passed through two high aspect-ratio cation exchange columns (AG50W X12), using dilute HCl as eluant based on the approach of James and Palmer (2000), and described in detail by Marschall *et al.* (2007) and Pogge von Strandmann *et al.* (2011). The Li fractions were measured using a Thermo Finnegan Neptune MC-ICP-MS, with sample-bracketing using a solution of NIST 8545 (Jeffcoate *et al.* 2004). Samples were analysed 2 or 3 times during the given sequence. Internal precision was typically better than \pm 0.2‰ (2s). The long-term reproducibility for the Bristol laboratory is \leq 0.3‰ (2s), based on analyses of silicate rock RMs BHVO-2 and BCR-2 over a period of four years (δ^7 Li = 4.7 \pm 0.2‰ n = 31 and δ^7 Li = 2.6 \pm 0.3‰ n = 18, respectively, all uncertainties 2s; Pogge von Strandmann *et al.* 2011).

442443444

<u>University of Bremen:</u>

- Values of δ^7 Li of the three tourmaline materials were determined in the Isotope Geochemistry
- 446 Laboratory at the MARUM Center for Marine Environmental Sciences, University of

Bremen. Sample digestion, separation and purification of lithium were modified after Moriguti and Nakamura (1998). Between 3 and 15 mg of crushed tourmaline sample were digested at 170°C in 2 ml HF/HNO₃ mixture (5:1) in steel-clad Teflon bombs, dried at 80°C, repeatedly re-dissolved in 2 ml 2M HNO₃ and dried to convert all fluorides into nitrates. The decomposed samples were finally dissolved in 4M HCl. For the schorl and elbaite materials five solution aliquots per sample were taken, each containing between 60 and 220 ng Li; the Li-poor dravite sample could only be analysed once. Each aliquot solution went through a three-step purification procedure using BioRad® AG 50WX8 (200-400 mesh) resin. The first step removed the trivalent matrix elements (e.g. rare earth elements) using BioRad® Bio-Spin columns with 1 ml of the cation-exchange resin and 4M HCl (for conditioning the resin and loading the sample) and 2.8M HCl (to elute Li) as reagents. The second step removed the majority of matrix elements (e.g. Ca, Mg, etc.) using BioRad® Poly-Prep columns with 1.4 ml of the cation-exchange resin and 0.15M HCl as reagent. In the final step, Na was separated using BioRad® Bio-Spin columns with 1 ml resin and 0.15M HCl followed by 0.5M HCl in 50% ethanol as reagents. Lithium must be quantitatively separated from the sample matrix, since the loss of only 1% of Li during column separation as well as the presence of Na can result in significant shifts in the Li isotope composition (James and Palmer 2000, Nishio and Nakai 2002, Jeffcoate et al. 2004). Li loss during column separation was monitored by testing the collected head and tail fractions of each separation step. The total Li loss was typically < 0.1% of total collected Li, and was thus insignificant. Reference materials NIST 8545 (LSVEC Li carbonate, Flesch et al. 1973), ZGI-TB-2 (clay shale), ZGI-GM (granite) and tourmaline IAEA-B-4 (powdered batch, Universität Bremen) were separated and analysed together with the samples as quality control materials. The Li blank input during the whole analytical procedure was less than 14 pg Li, which had no significant influence on the isotopic composition of the processed materials. Isotope analyses were performed on a MC-ICP-MS (Thermo Scientific Neptune Plus) using the stable introduction system together with a highefficiency x-cone (Hansen et al. 2017). Processed samples and QCMs as well as the unprocessed NIST 8545 were dissolved in 2% HNO₃, closely adjusted to 25 µg/L Li content and repeatedly analysed in the standard-sample bracketing mode using the unprocessed NIST 8545 as calibrant. The 2% HNO3 used for sample dissolution was measured as analytical baseline for correction. The determined Li isotope ratios are reported as delta-notation relative to NIST 8545. The processed NIST 8545 shows a δ^7 Li of -0.01 \pm 0.11‰ (2s, n = 4) indicating that no significant isotope fractionation occurred during the analytical procedure and confirming the long-term $\delta^7 \text{Li}$ value of $0.01 \pm 0.18\%$ (2s, n = 78). $\delta^7 \text{Li}$ values of ZGI-TB-2 (- $3.4 \pm 0.2\%$, 2s, n = 2) agree well with published values of ZGI-TB (-3.3 ± 0.4%, 2s; Romer et al. 2014). The ZGI-GM gives a δ^7 Li value of -0.7 ± 0.1% (2s, n = 2), that fits well with the published value of $-0.9 \pm 0.6\%$ (2s, n = 2) (Meixner et al. 2019). Tourmaline RM IAEA-B4 was also used as a quality control material, yielding a $\delta^7 \text{Li}$ of 4.3 \pm 0.3% (2s). Lin et al. (2019) reported a δ^7 Li value of 5.64 for the B4 tourmaline; here we note that the value reported for schorl and elbaite in that manuscript are likewise higher than our values based on four independent laboratories. The external reproducibility of silicate samples is generally \leq 0.5% (2s). The repeatability of the individual δ^7 Li values is reported as two standard deviations based on the five individually analysed sample aliquots.

447

448449

450

451

452

453

454455

456

457

458

459

460

461

462463

464

465

466

467468

469 470

471

472

473

474

475

476

477

478 479

480

481

482

483 484

485 486

487

488

Oxygen isotope ratios were determined by gas-source mass spectrometry using either laserfluorination or step-wise fluorination techniques in six independent laboratories: University of Wisconsin (Madison), the Open University (Milton Keynes), University of Göttingen, University of Cape Town, the Scottish Universities Environmental Research Centre SUERC (East Kilbride) and the National Environmental Isotope Facility of the British Geological Survey (Keyworth). Each laboratory analysed between one and four aliquots of grain fragments from each of the three tourmaline materials, and each analysis involved between one and four separate determinations. Additionally, all laboratories analysed the UWG-2 garnet RM (Valley et al. 1995) as a silicate traceability material. All labs reported δ^{18} O values; in addition, the Open University and University of Göttingen labs reported δ^{17} O results. Analytical technique descriptions for each of the participating labs are given below, a summary of the results is given in Table 6 and the compilation of all data is provided in electronic supplement Table 6. These tables also report the results obtained on the UWG-2 garnet traceability material; nearly all of the six participating gas source laboratories reported a mean value for UWG-2 which was in close agreement with the previously reported value of $\delta^{18}O_{SMOW} = 5.8$ (Valley et al. 1995). Table 6 also shows the previously published $\delta^{18}O_{SMOW}$ working values for the three Harvard tourmalines as reported by Dyar et al. (2001); for the dravite and elbaite materials good agreement is seen between these previous working values and the new results presented here. Finally, on table 6 we also report Δ^{17} O value for the Open University and Göttingen data sets, where $\Delta^{'17}O$ is defined as:

511512

513

492

493

494

495

496

497

498

499

500501

502

503

504

505

506

507

508

509

510

$$\Delta'^{17}O = 1000 \cdot \ln \left(\frac{\delta^{17}O}{1000} + 1 \right) - 0.528 \cdot 1000 \cdot \ln \left(\frac{\delta^{18}O}{1000} + 1 \right)$$
 eq. 4

514515

516517

518

with both, $\delta^{17}O$ and $\delta^{18}O$ on VSMOW scale. To ensure that $\delta^{17}O$ is on the VSMOW scale, our data are linked via the composition of UWG-2 garnet, taken as $\Delta^{'17}O = -0.062\%$, which is 0.01% lower than that of San Carlos olivine (Miller *et al.* 2020) that was measured relative to VSMOW2 and SLAP2 to be $\Delta^{'17}O = -0.052\%$ (mean of the determinations by Pack *et al.* 2016; Sharp *et al.* 2016; Wostbrock *et al.* 2020).

519520521

522

523

524

525526

527

528

529

530531

University of Wisconsin:

Oxygen isotope ratios were measured at the Department of Geoscience, University of Wisconsin-Madison. Aliquots of tourmaline weighing 1.9 to 3.3 mg were individually heated in a BrF5 atmosphere using a CO2 laser ($\lambda = 10.6 \, \mu m$) at a beam diameter of ~1 mm and a power of ~19 W. Evolved O2 was cleaned cryogenically, converted to CO2 on hot graphite, and analysed on mass stations 44, 45 and 46 using a Finnigan MAT 251 gas-source mass spectrometer. Values are reported in standard permil notation relative to VSMOW. The silicate RM UWG-2 (Valley *et al.* 1995) was analysed in the same analytical session as the tourmalines. UWG-2 is calibrated versus NBS-28 quartz ($\delta^{18}O = 9.59\%$, Hut 1987). Analyses of the UWG-2 garnet on the same day of analysis yielded $\delta^{18}O = 5.76 \pm 0.11\%$ (2SD, n = 4); tourmaline values were corrected by +0.04% to the published value of 5.80% for UWG-2, as recommended by Valley *et al.* (1995).

532533534

<u>University of Cape Town:</u>

535 Aliquots of tourmaline grains between 1.8 to 4.3 mg were laser-heated in a reaction cell with 536 BrF₅ (MIR 10-30 CO₂ laser, $\lambda = 10.6 \mu m$), with a spot diameter of 1 mm to 0.25 mm (start to finish, respectively) and between 1.5 and 15 W power. The released O2 was purified in cold 537 538 traps collected on 5 µm molecular sieve, and analysed offline as O₂ using a Thermo Delta XP 539 mass spectrometer using the mass stations 32, 33 and 34. Raw data were initially recalculated 540 to the VSMOW scale using the in-house reference Monastery garnet (Mon Gt; $\delta^{18}O$ = 541 5.38‰). Yields were calculated from inlet pressure to the mass spectrometer relative to that of 542 Mon Gt, assuming a constant volume of the inlet system. The analyses were run on two 543 separate sessions and yielded δ^{18} O values for the UWG-2 garnet of 5.67 and 5.69 and 5.81 544 and 5.87‰. Data were normalized to the accepted value for UWG-2 of 5.80‰ (Valley et al. 1995) and expressed in the permil notation relative to VSMOW. Full details of the method are 545 546 given in Harris and Vogeli (2010).

547548

University of Göttingen:

Aliquots of tourmaline weighing ~2 mg were heated in a BrF₅ atmosphere by laser (λ = 10.6 µm). Evolved O₂ was cleaned cryogenically and by gas chromatography and was measured in a Thermo Finnigan Mat 253 gas source mass spectrometer (for details see Pack *et al.* 2016). Values for δ^{17} O and δ^{18} O are reported in standard permil notation relative to VSMOW. The external reproducibility (1s) was 0.04‰ for δ^{17} O, 0.08‰ for δ^{18} O, and 0.009‰ for Δ^{*17} O (note that the uncertainties for δ^{17} O and δ^{18} O are highly correlated; see also Wostbrock *et al.* 2020).

556557

Open University, Milton Keynes

558 Aliquots of tourmaline weighing 2.0 to 2.1 mg were heated in a BrF₅ atmosphere by laser ($\lambda =$ 559 10.6 μm) ramped up to ~15W power. Evolved O₂ was prepared through a two-stage cryogenic 560 purification process with an intermediate hot (110°C) KBr reactor. The purified O₂ gas was cryofocused at the entrance of the analyser using zeolite molecular sieve at -196°C before 561 562 being analysed by gas-source mass spectrometer (Thermo Finnigan MAT 253). Details of 563 analytical procedures are given in Miller et al. (1999). Values for δ^{17} O and δ^{18} O are reported 564 in standard ‰ notation relative to VSMOW. Typical long-term external reproducibility is ± 0.052% for δ^{17} O; $\pm 0.093\%$ for δ^{18} O; $\pm 0.017\%$ for Δ^{17} O (2s) (Greenwood *et al.* 2015). 565 Analyses of UWG-2 yielded $5.75 \pm 0.06\%$ (1s, n = 4). 566

567568

SUERC East Kilbride

569 Aliquots of tourmaline weighing between 1.7 to 2.9 milligrams of tourmaline, and between 570 1.4 and 3.0 milligrams of UWG-2 garnet, were pre-fluorinated overnight, under vacuum in 571 the sample chamber. Samples were then individually heated in a ClF₃ atmosphere by laser 572 (SYNRAD J48-2 CO₂ laser $\lambda = 10.6 \mu m$), following the method of Sharp (1990). The evolved 573 O₂ was cleaned cryogenically, and passed through an on-line hot mercury diffusion pump, 574 before being converted to CO₂ on hot graphite, and analysed by gas-source mass spectrometer (VG SIRA2). Values are reported in standard permil notation relative to VSMOW. Analyses 575 576 of the UWG-2 garnet during the analytical session yielded 5.75 \pm 0.08% (1s, n = 9). Values 577 were corrected by 0.04% to the accepted value of 5.80 for UWG-2 (Valley et al. 1995).

BGS Keyworth:

The tourmalines, weighing between 6.1 and 6.6 mg, were powdered, transferred to pure nickel reaction vessels, and furnace-heated to 700°C in an excess of BrF₅ for an extended period (> 16 h). The evolved O₂ was cleaned cryogenically, converted to CO₂ on hot graphite, and collected under liquid N₂. Oxygen isotope analyses were conducted with a Thermo Finnigan MAT 253 dual inlet mass spectrometer. Values are reported in standard δ -notation in permil relative to VSMOW calibrated using NBS28 quartz, which has an assigned composition of $\delta^{18}O = 9.59\%$ (Hut 1987). Analyses of the UWG-2 garnet during the session yielded 5.49 \pm 0.46% (1s, n = 3). Values were corrected by 0.31% to the accepted value of 5.80% for UWG-2 (Valley *et al.* 1995). It is noted that the Keyworth laboratory does not normally run high temperature minerals, and fluorination was conducted at a temperature well above the typical 500°C used in this facility for biogenic silica. This deviation for the Keyworth validated operating protocol may have contributed to the somewhat lower mean $\delta^{18}O$ value (-0.3%; n = 3) determined on the UWG-2 garnet traceability material.

Discussion

Table 7 summarizes the best available values for stable isotope ratios of the three Harvard tourmaline materials.

Major element compositions

With respect to the major element compositions of the three Harvard tourmaline RMs, we believe the best estimates of their major element compositions and their inter-fragment variabilities are provided by the grand means of two EPMA data sets presented in Table 1. In general, the grand means reported from Potsdam and Madison agree well, though biases outside the reported repeatability are also visible for some elements. Both sets of EPMA results provide data that characterize the composition of the tourmalines. We note that the values for B composition determined by EPMA are in excellent agreement with earlier non-EPMA technique data (Dyar *et al.* 2001). However, due to different analytical EPMA protocols further examinations of all three tourmaline RMs will be necessary in order to establish recommended values. For the time being, the grand means reported in Table 1 should be considered as working values, subject to possible future refinement.

Working values for lithium concentrations

Based on the observed repeatabilities of our SIMS data as compared to both the (presumably) homogeneous NIST 610 silicate glass and the internal precision of the individual SIMS measurements (Table 2), it appears that significant variability in the Li₂O contents are present in all three materials. Furthermore, our "current best estimate" values for Li contents (Table 7) are derived from a SIMS calibration based on the NIST 610 glass; as such, we do not have a matrix matched calibration. We conclude that the Li content values presented in Table 7 should only be used as rough indicators, and that any values calibrated using these materials should employ multiple grains so as to suppress issues related to the observed sample heterogeneity.

Recommended values for lithium isotopes

A comparison of the δ^7 Li values determined by the four laboratories (Table 5) shows good agreement for all three RMs, the only noteworthy observation being the consistently lower δ⁷Li values reported in the University of Maryland data set, which differs by roughly 1‰ from the results reported by Bremen, Bristol and Woods Hole. The source of this phenomenon is unclear, particularly in view of the detailed quality assurance plans implemented by all four bulk analyses laboratories. In total there are eight repeated pairs of data in our full data set (Table 5), and these have on average a difference of only 0.38% between the members of the pairs. Equally, the overall repeatabilities of the SIMS homogeneity assessments were better than \pm 0.8% (1s) for both of the Li-rich materials (Table 3). Hence, both the repeatability of our analytical methods and the homogeneity observed by SIMS are significantly better than the observed spread in the result. Based on these observations, we suggest that the median δ^7 Li values based on the individual (n = 6 or 7) bulk δ^7 Li determinations represent the best possible estimates of the true value of the three materials. These are reported in Table 5 and their assigned uncertainties are the repeatabilities of the complete set of determinations divided by sqrt(n-1). We note that our results for schorl and elbaite are roughly 0.9% lower than those reported by Lin et al. (2019) (see table 5).

Recommended values for oxygen isotopes

The results of 33 δ^{18} O laser and step-wise fluorination determinations reported by six independent laboratories show excellent agreement for all three of the tourmaline RMs (Table 6). The internal precision of individual analyses is better than \pm 0.1% (1s) for all of the gas source data (electronic supplement Table 6). With regard to the homogeneity at the picogram sampling scale, our SIMS data (Table 4) yielded repeatabilities similar to that obtained on the NIST 610 silicate glass, which we presume to be isotopically homogeneous at the SIMS sampling scale. We therefore conclude that the recommended δ^{18} O values reported in Table 7 can be used to calibrate *in situ* oxygen isotope ratio analyses at \pm 0.3% (1s) data quality or better. Finally, we note that the new data are in good agreement with the δ^{18} O values for dravite and elbaite reported in Dyar *et al.* (2001) whereas in the case of schorl there is a difference of 0.66% between our gas-source data mean and that from the earlier publication (see Table 6). As our data are based on multiple results reported by six independent laboratories, we recommend that the δ^{18} O and δ^{17} O and δ^{17} O values reported in Table 7 should be used for calibrating future studies.

SIMS Matrix Effects

In the case of the three Harvard tourmaline RMs it is not possible for us to say anything with regards to SIMS matrix effects related to Li concentration determinations as we do not have any independently determined value for the three materials in which we have high confidence. Equally, in the case of ⁷Li/⁶Li determinations we cannot conclude anything meaningful regarding a chemical matrix effect. The large differences in Li concentrations mean that each of the three RMs had to be run under distinct analytical conditions, preventing any direct comparison. The only thing that can be said concerning a matrix effect is through comparing the schorl RM and the concurrently run NIST 610 silicate glass, which was used as a drift

monitor. Kasemann *et al.* (2005) published a solution MC-ICP-MS value of $\delta^7 \text{Li}_{\text{L-SVEC}} = 32.50 \pm 0.02$ for NIST 610, which is equivalent to an absolute isotope ratio of $^7 \text{Li}/^6 \text{Li} = 12.5686$ (see eq. 3). During our homogeneity testing we obtained on n = 8 measurements $^7 \text{Li}/^6 \text{Li} = 11.8166$ for NIST 610 (Table 3), corresponding to an Instrumental Mass Fractionation (IMF) of 11.8166/12.5686 = 0.94016. For the concurrently analysed schorl, the IMF value is 0.94993, based on our recommended $\delta^7 \text{Li} = 5.52$ (Table 7) and the observed average $^7 \text{Li}/^6 \text{Li} = 11.6273$ (Table 3). Comparison of these IMF values indicates a difference of *circa* 10% between the schorl and silicate glass matrix. Similar to what has already been demonstrated for SIMS boron isotope data (e.g., Rosner *et al.* 2008), the use of NIST silicate glass RMs (61x series) for calibrating SIMS lithium isotope measurements of tourmaline leads to a grossly biased result.

During our SIMS ¹⁸O/¹⁶O homogeneity test run we ran all three of the Harvard tourmaline RMs as well as NIST 610 glass (as drift monitor) during a single analytical sequence under identical analytical conditions. This allows us to evaluate the impact of the various matrices on the SIMS IMF value. For the tourmaline RMs we used the grand mean δ^{18} O values reported in Table 6 in conjunction with the absolute ratio for SMOW of 18 O/ 16 O = 0.00200520 (Baertschi 1976). In the case of NIST 610 silicate glass we used the value reported by Kasemann et al. (2001) of $\delta^{18}O_{SMOW} = 10.91$ (see eq. 1 for conversion to absolute isotope ratio). The resulting IMF values for each of these four materials are reported in Table 4. Among the three tourmaline RMs the maximum difference in IMF is 1.9%, as seen between schorl and elbaite, with dravite yielding an IMF intermediate between the two. These differences in IMF are large compared to the analytical uncertainties and are similar to variations in IMF reported for oxygen isotope ratio determinations on tourmaline by Marger et al. (2019); that earlier work reported that tourmalines having low iron contents (e.g., elbaite) tend to measure comparatively high ¹⁸O^{-/16}O⁻ SIMS results. This observation suggests that, despite the low uncertainties of the gas-source data and the good repeatability of our SIMS method, the determination of δ^{18} O in natural tournalines at precision levels better than 0.5% will be difficult except where there is a close chemical match between the unknown sample and one of these RMs, as has been shown for garnet and other minerals (Valley and Kita 2009, Page et al. 2010). For the case of NIST 610, the IMF was biased by between 3% and 5% relative to the dravite and schorl RMs, respectively. This confirms that, at least in the case of SIMS, the use of a silicate glass calibrant is inappropriate for δ^{18} O determinations on tourmaline.

Material Availability

667

668669

670671

672

673

674675

676

677

678679

680

681

682

683

684

685

686

687 688

689

690

691

692

693694

695

696

697

698699

700701

702703

704

705

706

707

708

709

710

Since 2014 the three Harvard tourmalines RMs described here have been distributed through IAGeo Limited (www.iageo.com), and it is expected this arrangement will continue on into the future. Vials containing ca. 100 mg of tourmaline (samples HMGM #98144.1, HMGM # 112566.1 and HMGM #108796.1) are therefore readily available to the global user community. In light of the large number of splits that were produced of each of these materials (128 or 512 units) in conjunction with past levels of demand, it is reasonable to expect this resource will last for at least two decades into the future.

Acknowledgements

711712

- 713 MW & RT acknowledge F. Couffignal for his skills at operating the SIMS instrument and U.
- 714 Dittmann for excellent SIMS sample preparation work (Potsdam). CH thanks Sherissa
- Roopnarain (Cape Town) for help with mass spectrometry. RH acknowledges the support and
- advice of R. Rudnick, W.F. McDonough and R. Ash in the Maryland laboratory. R. Przybilla
- and D. Kohl (University of Göttingen) are thanked for preparing and analysing the samples
- and keeping the laboratory running. JWV and MJS (University of Wisconsin) are supported
- by the U.S. National Science Foundation (EAR-1524336) and Department of Energy (DE-
- 720 FG02-93-ER14389). MR acknowledges the use of the NSF-supported WHOI ICP-MS facility
- and thanks Larry Ball and Jerzy Blusztajn for their assistance. Analyses at Bristol were
- supported by NERC grant NER/C510983/1. We also thank two reviewers who provided
- 722 valuable suggestions for improving this manuscript. Finally, we wish to then! the Herward
- valuable suggestions for improving this manuscript. Finally, we wish to thank the Harvard
- Museum for ongoing support of such projects.

725

726 727

References

728

- 729 **Armstrong J.T. (1995)**
- 730 CITZAF: A package of correction programs for the quantitative electron microbeam X-ray
- analysis of thick polished materials, thin films, and particles. Microbeam Analysis, 4, 177-
- 732 200.

733

- 734 Baertschi P. (1976)
- Absolute ¹⁸O content of Standard Mean Ocean Water. Earth and Planetary Science Letters,
- 736 31, 341-344. doi: 10.1016/0012-821X(76)90115-1

737

- 738 **Barkan E., Luz B. (2005)**
- High precision measurements of ¹⁷O/¹⁶O and ¹⁸O/¹⁶O ratios in H₂O. Rapid Communications
- 740 in Mass Spectrometry 19, 3737-3742. doi: /10.1002/rcm.2250

741

742 Bell D.R., Hervig R.L., Buseck P.R., Aulbach S. (2009)

- 743 Lithium isotope analysis of olivine by SIMS: Calibration of a matrix effect and application to
- magmatic phenocrysts. Chemical Geology, 258, 5-16. doi: 10.1016/j.chemgeo.2008.10.008

745

- 746 **Bouman C., Elliott T., Vroon P.Z. (2004)**
- 747 Lithium inputs to subduction zones. Chemical Geology, 212, 59-79. doi:
- 748 10.1016/j.chemgeo.2004.08.004

749

- 750 Brand W.A., Coplen T.B., Vogl J., Rosner M., Prohaska T. (2014)
- Assessment of international reference materials for isotope-ratio analysis (IUPAC Technical
- 752 Report). Pure and Applied Chemistry, 425-467. doi: 10.1515/pac-2013-1023

753

754 Chan L.-H., Frey F.A. (2003)

- 755 Lithium isotope geochemistry of the Hawaiian plume: results from the Hawaii Scientific
- 756 Drilling Project and Koolau Volcano. Geochemistry, Geophysics, Geosystems, 4(3), 8707.
- 757 doi:10.1029/2002GC000365

- 759 **Coplen T.B. (2011)**
- Report of stable isotopic composition Reference Material LSVEC (carbon and lithium
- isotopes in lithium carbonate). United States Geological Survey Reston Stable Isotope
- 762 Laboratory, 3p.

763

- 764 Dyar M.D., Wiedenbeck M., Robertson D., Cross L.R., Delaney J.S., Ferguson K.,
- 765 Francis C.A., Grew E.S., Guidotti C.V., Hervig R.L., Hughes J.M., Husler J., Leeman
- 766 W., McGuire A.V., Rhede D., Rothe H., Paul R.L., Richards I., Yates M. (2001)
- Reference minerals for microanalysis of light elements. Geostandards Newsletter, 25/2, 441-
- 768 463. doi: 10.1111/j.1751-908X.2001.tb00616.x

769

- 770 Flesch G.D., Anderson A.R., Svec H.J. (1973)
- A secondary isotopic standard for ⁶Li/⁷Li determinations. International Journal of Mass
- 772 Spectrometry and Ion Physics, 12, 265-272.

773

- 774 Frondel C., Biedl A., Ito J. (1966)
- New type of ferric iron tourmaline. American Mineralogist, 51, 1501-1505.

776

- 777 Gonfiantini R., Tonarini S., Gröning M., Adorni-Braccesi A., Al-Ammar A.S., Astner
- 778 M., Bächler S., Barnes R.M., Bassett R.L., Cocherie A., Deyhle A., Dini A., Ferrara G.,
- Gaillardet J., Grimm J., Guerrot C., Krähenbühl U., Layne G., Lemarchand D.,
- 780 Meixner A., Northington D.J., Pennisi M., Reitznerová E., Rodushkin I., Sugiura N.,
- 781 Surberg R., Tonn S., Wiedenbeck M., Wunderli S., Xiao Y., Zack T. (2003)
- 782 Intercomparison of boron isotope and concentration measurements. Part II: Evaluation of
- 783 results. Geostandards Newsletter, 27/1, 41-57. doi: 10.1111/j.1751-908X.2003.tb00711.x

784

- 785 Greenwood R.C., Barrat J.-A., Scott E.R.D., Haack H., Buchanan P.C., Franchi I.A.,
- 786 Yamaguchi A., Johnson D., Bevan A.W.R., Burbine T.H. (2015)
- 787 Geochemistry and oxygen isotope composition of main-group pallasites and olivine-rich
- 788 clasts in mesosiderites: Implications for the 'Great Dunite Shortage' and HED-mesosiderite
- connection. Geochimica et Cosmochimica Acta, 169, 115-136. doi: 0.1016/j.gca.2015.07.023

790

- 791 Halama R., McDonough W.F., Rudnick R.L., Bell K. (2008)
- 792 Tracking the lithium isotopic evolution of the mantle using carbonatites. Earth and Planetary
- 793 Science Letters, 265,726-742. doi: 10.1016/j.epsl.2007.11.007

794

- 795 Hansen C.T., Meixner A., Kasemann S. A., Bach W. (2017)
- New insight on Li and B isotope fractionation during serpentinization derived from batch
- reaction investigations. Geochimica et Cosmochimica Acta, 217, 51–79. doi:
- 798 10.1016/j.gca.2017.08.014

- 800 Harms A.V., Assonov A. (2018)
- 801 Reference sheet reference material LSVEC (Li-carbonate) Reference Material for Li-isotope
- ratio. International Atomic Energy Agency, 5p.

- 804 Harris C., Vogeli J. (2010)
- Oxygen isotope composition of garnet in the Peninsula Granite, Cape Granite Suite, South
- 806 Africa: Constraints on melting and emplacement mechanisms. South African Journal of
- 807 Geology, 113, 385-396. doi: 10.2113/gssajg.113.4.401

808

- Henry D.J., Novák M., Hawthorne F.C., Ertl A., Dutrow B.L., Uher P., Pezzotta F.
- 810 (2011)
- Nomenclature of the tourmaline supergroup minerals. American Mineralogist, 96, 895–913.
- 812 doi: 10.2138/am,2011.3636

813

- Herwartz D., Pack A., Krylov D., Xiao Y., Muehlenbachs K., Sengupta S., Di Rocco T.
- 815 (2015)
- Revealing the climate of 'snowball Earth' from Δ^{17} O systematics of hydrothermal rocks.
- Proceedings of the National Academy of Sciences, 112, 5337-5341. doi:
- 818 10.1073/pnas.1422887112

819

- 820 **Hut G. (1987)**
- 821 Consultants' group meeting on stable isotope reference samples for geochemical and
- 822 hydrological investigations. International Atomic Energy Agency (IAEA). International
- 823 Atomic Energy Agency (IAEA), Vienna, p. 49

824

- 825 **Hutchinson R.W., Claus R.J. (1956)**
- Pegmatite deposits, Alto Ligonha, Portuguese East Africa. Economic Geology, 51, 575-780.

827

- 828 **James R.H., Palmer M.R. (2000)**
- The lithium isotope composition of international rock standards. Chemical Geology, 166,
- 830 319-326. doi: 10.1016/S0009-2541(99)00217-X

831

- 832 Jeffcoate A.B., Elliott T., Thomas A., Bouman C. (2004)
- Precise, small sample size determinations of lithium isotopic compositions of geological
- reference materials and modern seawater by MC-ICP-MS. Geostandards and Geoanalytical
- 835 Research, 28, 161-172. doi: 10.1111/j.1751-908X.2004.tb01053.x

836

- Jochum K.-P., Weis U., Stoll B., Kuzmin D., Yang Q., Raczek I., Jakob D.E., Stracke A.,
- 838 Birbaum K., Frick D.A., Guenther D., Enzweiler J. (2011)
- 839 Determination of Reference Values for NIST SRM 610–617 Glasses Following ISO
- Guidelines. Geostandards and Geoanalytical Research, 35/4, 397-429. doi: 10.1111/j.1751-
- 841 908X.2011.00120.x

- 843 Kasemann S., Meixner A., Rocholl A., Vennemann T., Rosner M., Schmitt A.K.,
- 844 **Wiedenbeck M. (2001)**

- Boron and oxygen isotope composition of certified reference materials NIST 610/612 and
- reference materials JB-2 and JR-2. Geostandards Newsletter, 25/2-3, 405-416. doi:
- 847 10.1111/j.1751-908X.2001.tb00615.x

- 849 Kasemann S.A., Jeffcoate A.B., Elliot T. (2005)
- Lithium isotope composition of basalt glass reference material. Analytical Chemistry, 77,
- 851 5251-5257. doi: 10.1021/ac048178h

852

- 853 Kutzschbach M., Wunder B., Trumbull R.B., Rocholl A., Meixner A., Heinrich W.
- 854 **(2017**)
- An experimental approach to quantify the effect of tetrahedral boron in tourmaline on the
- boron isotope fractionation between tourmaline and fluid. American Mineralogist, 102, 2505-
- 857 2511. doi: 10.2138/am-2017-6127

858

- 859 Leeman W.P., Tonarini S. (2001)
- 860 Boron isotopic analysis of proposed borosilicate mineral reference samples. Geostandards
- 861 Newsletter, 25/2, 441-403. doi: 10.1111/j.1751-908X.2001.tb00614.x

862

- Li W., Ni B., Jin D., Zhang Q. (1988) Measurement of the absolute abundance of oxygen-17
- in V-SMOW. Chinese Science Bulletin, English Translation, 33, 1610-1613. doi:
- 865 10.1360/sb1988-33-19-1610

866

- 867 Lin J., Liu Y., Hu Z., Chen W., Zhang C., Zhao K., Jin X. (2019)
- Accurate analysis of Li isotopes in tourmalines by LA-MC-ICP-MS under "wet" conditions
- with non-matrix-matched calibration. Journal of Analytical Atomic Spectrometry, 34, 1145-
- 870 1153. doi: 10.1039/C9JA00013E

871

- 872 Ludwig T., Marschall H.R., Pogge von Strandmann P.A.E., Shabaga B.M., Fayek M.,
- 873 **Hawthorne F.C. (2011)**
- A secondary ion mass spectrometry (SIMS) re-evaluation of B and Li isotopic compositions
- of Cu-bearing elbaite from three global localities. Mineralogical Magazine, 75, 2485–2494.
- 876 doi: 10.1180/minmag.2011.075.4.2485

877

- 878 Marger K., Luisier C., Baumgartner L.P., Putlitz B., Dutrow B.L., Bouvier A.-S., Dini
- 879 **A. (2019)**
- Origin of Monte Rosa whiteschist from in-situ tourmaline and quartz oxygen isotope analysis
- by SIMS using new tourmaline reference materials. American Mineralogist, 104, 1503-1520.
- 882 doi: 10.2138/am-2019-7012

883

- Marger K., Harlaux M., Rielli A., Baumgartner L.P., Dini A., Dutrow B.L., Bouvier A.-
- 885 **S. (2020)**
- Development and re-evaluation of tourmaline reference materials for *in* situ measurement of
- 887 boron δ values by Secondary Ion Mass Spectrometry. Geostandards and Geoanalytical
- 888 Research, 44/3, 593-615. doi: 10.1111/ggr.12326

- 890 Marks M.A.W., Rudnick R.L., McCammon C., Vennemann T., Markl G. (2007)
- Arrested kinetic Li isotope fractionation at the margin of the Ilímaussaq complex, South
- 892 Greenland: Evidence for open-system processes during final cooling of Peralkaline igneous
- 893 rocks. Chemical Geology, 246, 207-230. doi: 10.1016/j.chemgeo.2007.10.001

- 895 Marschall H.R., Jiang S.-Y. (2011)
- 896 Tourmaline Isotopes: No Element Left Behind. Elements, 7, 313-319. doi:
- 897 10.2113/gselements.7.5.313

898

- 899 Marschall H.R., Foster G.L. (2018)
- Boron isotopes the fifth element. Advances in Geochemistry, 7, 249-272.

901

- 902 Marschall H.R., Pogge von Strandmann P.A.E., Seitz H.-M., Elliott T., Niu Y. (2007)
- The lithium isotopic composition of orogenic eclogites and deep subducted slabs. Earth and
- 904 Planetary Science Letters, 262, 563-580. doi: 10.1016/j.epsl.2007.08.005

905

- 906 Matthews A., Putlitz B., Hamiel Y., Hervig R.L. (2003)
- Volatile transport during the crystallization of anatectic melts: Oxygen, boron and hydrogen
- stable isotope study on the metamorphic complex of Naxos, Greece. Geochimica et
- 909 Cosmochimica Acta, 67, 3145-3163. doi: 10.1016/S0016-7037(02)01168-7

910

- 911 Meixner A., Sarchi C., Lucassen F., Becchio R., Caffe P.J., Lindsay J., Rosner M.,
- 912 Kasemann S.A. (2019)
- 913 Lithium concentrations and isotope signatures of Palaeozoic basement rocks and Cenozoic
- volcanic rocks from the Central Andean arc and back-arc. Mineralium Deposita, 55, 1071–
- 915 1084. doi: 10.1007/s00126-019-00915-2

916

- 917 Míková J., Košler J., Wiedenbeck M. (2014)
- 918 Matrix effects during laser ablation MC ICP-MS analysis of boron isotopes in tourmaline.
- Journal of Analytical and Atomic Spectrometry, 29, 903-914. doi: 10.1039/C3JA50241D

920

- 921 Miller M.F., Franchi I.A., Sexton A., Pillinger C.T. (1999)
- High precision $\Delta 170$ isotope measurements of oxygen from silicates and other oxides:
- 923 Method and applications. Rapid Communications in Mass Spectrometry, 13, 1211-1217.
- 924 doi: 10.1002/(SICI)1097-0231(19990715)13:13<1211::AID-RCM576>3.3.CO;2-D

925

- 926 Miller M.F., Pack A., Bindeman I.N., Greenwood R.C. (2020)
- Standardizing the reporting of Δ^{17} O data from high precision oxygen triple-isotope ratio
- measurements of silicate rocks and minerals. Chemical Geology, 532, 119332. doi:
- 929 10.1016/j.chemgeo.2019.119332

- 931 Moriguti T., Nakamura E. (1998)
- Across-arc variation of Li isotopes in lavas and implications for crust/mantle recycling at
- 933 subduction zones. Earth Planetary Science Letters, 163, 167-174. doi: 10.1016/S0012-
- 934 821X(98)00184-8

935	
936	Nishio Y., Nakai S. (2002)
937	Accurate and precise lithium isotopic determinations of igneous rock samples using multi-
938	collector inductively coupled plasma mass spectrometry. Analytica Chimica Acta, 456, 271-
939	281. doi: 10.1016/S0003-2670(02)00042-9
940	
941	Pack A., Herwartz D. (2014)
942	The triple oxygen isotope composition of the Earth mantle and understanding Δ^{17} O variations
943	in terrestrial rocks and minerals. Earth and Planetary Science Letters 390, 138-145. doi:
944	10.1016/j.epsl.2014.01.017
945	
946	Pack A., Tanaka R., Hering M., Sengupta S., Peters S., Nakamura E. (2016)
947	The oxygen isotope composition of San Carlos olivine on the VSMOW2-SLAP2 scale. Rapid
948	Communications in Mass Spectrometry, 30/13, 1495-1504. doi: 10.1002/rcm.7582
949	
950	Page F.Z., Kita N.T., Valley J.W. (2010)
951	Ion microprobe analysis of oxygen isotopes in garnets of complex chemistry. Chemical
952	Geology, 270, 9-19. doi: 10.1016/j.chemgeo.2009.11.001
953	
954	Pogge von Strandmann P.A.E., Elliott T., Marschall H.R., Coath C., Lai YJ., Jeffcoate
955	A.B., Ionov D.A. (2011)
956	Variations of Li and Mg isotope ratios in bulk chondrites and mantle xenoliths. Geochimica et
957	Cosmochimica Acta, 75, 5247-5268. doi: 10.1016/j.gca.2011.06.026
958	
959	Qi H.P., Taylor P.D.P, Berglund M., De Bievre P. (1997)
960	Calibrated measurements of the isotopic and atomic weight of the natural Li isotopic
961	reference material IRMM-016. International Journal of Mass Spectrometry and Ion Processes,
962	171, 263-268. Doi: 10.1016/S0168-1176(97)00125-0
963	
964	Romer R.L., Meixner A., Hahne K. (2014)
965	Lithium and boron isotopic composition of sedimentary rocks — The role of source history
966	and depositional environment. A 250Ma record from the Cadomian orogeny to the Variscan
967	orogeny. Gondwana Research, 26, 1093–1110. doi: 10.1016/j.gr.2013.08.015
968	
969	Rosner M., Ball L., Peucker-Ehrenbrink B., Blusztajn J., Bach W., Erzinger J. (2007)
970	A simplified, accurate and fast method for Li isotope analysis of rocks and fluids, and d ⁷ Li
971	values of seawater and rock reference materials. Geostandards and Geoanalytical Research,
972	31/2, 77-88. doi: 10.1111/j.1751-908X.2007.00843.x
973	
974	Rosner M., Wiedenbeck M., Ludwig T. (2008)
975	Composition-induced variations in SIMS instrumental mass fractionation during boron
976	isotope ratio measurements of silicate glasses. Geostandards and Geoanalytical Research,

Rudnick R.L., Tomascak P.B., Heather B.N., Gardner L.R. (2004)

32/1, 27-38. doi: 10.1111/j.1751-908X.2008.00875.x

977

- 980 Extreme lithium isotopic fractionation during continental weathering revealed in saprolites
- 981 from South Carolina. Chemical Geology, 212, 45-57. doi: 10.1016/j.chemgeo.2004.08.008

- 983 **Ryan J.G., Langmuir C.H. (1987)**
- The systematics of lithium abundances in young volcanic rocks. Geochimica et
- 985 Cosmochimica Acta., 51, 1727-1741. doi: 10.1016/0016-7037(87)90351-6

986

- 987 **Sharp Z.D. (1990)**
- A laser-based microanalytical method for the in-situ determination of oxygen isotope ratios of
- 989 silicates and oxides. Geochimica et Cosmochimica Acta, 54, 1353-1357. doi: 10.1016/0016-
- 990 7037(90)90160-M

991

- 992 Sharp Z.D., Gibbons J.A., Maltsev O., Atudorei V., Pack A., Sengupta S., Shock E.L.,
- 993 Knauth L.P. (2016)
- A calibration of the triple oxygen isotope fractionation in the SiO2-H2O system and
- applications to natural samples. Geochimica et Cosmochimica Acta, 186, 105-119. doi:
- 996 10.1016/j.gca.2016.04.047

997

- 998 Siegel K., Wagner T., Trumbull R.B., Jonsson E., Matalin G., Wälle M., Heinrich C.A.
- 999 (2016)
- Stable isotope (B,H,O) and mineral-chemistry constraints on the magmatic to hydrothermal
- evolution of the Varutrask rare-element pegmatite (northern Sweden). Chemical Geology,
- 1002 421, 1-16. doi: 10.1016/j.chemgeo.2015.11.025

1003

- 1004 Slack J.F., Trumbull R.B. (2011)
- Tourmaline as a recorder of ore-forming processes. Elements, 7, 321-326. doi:
- 1006 10.2113/gselements.7.5.321

1007

- 1008 **Taylor B.E., Palmer M.R., Slack J.F. (1999)**
- 1009 Mineralizing fluids in the Kidd Creek massive sulfide deposit, Ontario: evidence from
- oxygen, hydrogen, and boron isotopes in tourmaline. Economic Geology, Monograph 10,
- 1011 389-414.

1012

- 1013 Teng F.-Z., McDonough W.F., Rudnick R.L., Dalpé C., Tomascak P.B., Chappell B.W.,
- 1014 Gao S. (2004)
- 1015 Lithium isotopic composition and concentration of the upper continental crust. Geochimica et
- 1016 Cosmochimica Acta, 68, 4167-4178. doi: 10.1016/j.gca.2004.03.031

1017

- 1018 **Tomascak P.B. (2004)**
- Developments in the understanding and application of lithium isotopes in the Earth and
- Planetary sciences In: C.M. Johnson, B.A. Beard and F. Albarède (Eds.) Geochemistry of
- Non-traditional Stable Isotopes. Reviews in Mineralogy and Geochemistry 55, 153–195. doi:
- 1022 10.2138/gsrmg.55.1.153

1023

1024 Tomascak P.B., Carlson R.W., Shirey S.B. (1999)

- 1025 Accurate and precise determination of Li isotopic compositions by multi-collector sector ICP-
- 1026 MS. Chemical Geology, 158, 145-154. doi: 10.1016/S0009-2541(99)00022-4

- 1028 Tomascak P.B., Magna T., Dohmen R. (2016)
- 1029 Advances in Lithium Isotope Geochemistry. Advances in Geochemistry 7, Springer,
- 1030 Heidelberg, 195 pp. ISBN: 978-3-319-01430-2

1031

- 1032 Tonarini S., Pennisi M., Adorni-Braccesi A., Dini A., Ferrara G., Gonfiantini R.,
- 1033 Wiedenbeck M., Gröning M. (2003)
- 1034 Intercomparison of boron isotope concentration measurements. Part I: Selection, preparation
- 1035 and homogeneity tests of the intercomparison materials. Geostandards Newsletter, 27/1, 21-
- 1036 39. doi: 10.1111/j.1751-908X.2003.tb00710.x

1037

- 1038 Valley J.W. (2003)
- 1039 Oxygen isotopes in zircon. Reviews in Mineralogy 53, 343–385. doi: 10.2113/0530327

1040

- 1041 Valley J.W., Cole D., eds. (2001)
- 1042 Stable isotope geochemistry. Reviews in Mineralogy 43, 531 pp. ISBN: 0-939950-55-3

1043

- 1044 Valley J.W., Kita N.T. (2009)
- 1045 In situ Oxygen Isotope Geochemistry by Ion Microprobe, In: Fayek M. (ed.) MAC Short
- 1046 Course: Secondary Ion Mass Spectrometry in the Earth Sciences, 41, 19-63.

1047

- 1048 Valley J.W., Kitchen N., Kohn M.J., Niendorf C.R., Spicuzza J.J. (1995)
- 1049 UWG-2, a garnet standard for oxygen isotope ratios: Strategies for high precision and
- accuracy with laser heating. Geochimica et Cosmochimica Acta, 59, 5223-5231. doi: 1050
- 1051 10.1016/0016-7037(95)00386-X

1052

- 1053 Wostbrock J.A., Cano E.J., Sharp Z.D. (2020)
- 1054 An internally consistent triple oxygen isotope calibration of standards for silicates, carbonates
- 1055 and air relative to VSMOW2 and SLAP2, Chemical Geology, 533, 119432. doi:
- 1056 10.1016/j.chemgeo.2019.119432

1057

1058 1059

Figure Caption 1060

1061

1063 1064

Figure 1. Al-Fe-Mg diagram (molar proportions) showing the composition of the three 1062 Harvard tourmaline RMs investigated by this study (see Table 1). The positions of some of the more common tourmaline end members as well as that of the "B4" tourmaline RM 1065 (Tonarini et al. 2003) are also indicated. We point the reader to Marger et al. (2019, 2020) for other recent efforts to characterize alternative tourmaline isotope calibration 1066 1067 materials.

1069 **List of Tables** 1070 1071 Table 1: Major element compositions based on EPMA. Table 2: Summary of SIMS homogeneity tests for lithium concentration and new working 1072 1073 values. 1074 Table 3: Summary of SIMS homogeneity tests for lithium isotope ratios. Table 4: Summary of SIMS homogeneity tests for oxygen isotope ratios. 1075 Table 5: Summary of results of δ^7 Li_L-svec by solution ICP mass spectrometry. 1076 1077 Table 6: Summary results of oxygen-isotope analyses by gas source mass spectrometry. 1078 Table 7: Compilation of reference values for the three Harvard tourmaline materials. 1079 1080 1081 **List of Electronic Supplement Tables** 1082 1083 ES Table 1: Microprobe analyses of tourmaline reference materials, complete data set. 1084 ES Table 2: SIMS Li-concentration homogeneity test results, complete data set. 1085 ES Table 3: SIMS Li-isotope homogeneity test, complete data set. 1086 ES Table 4: SIMS oxygen isotope homogeneity test, complete data set. 1087 ES Table 5: Wet chemical lithium isotope ratio results, complete data set. 1088 ES Table 6: Gas source oxygen isotope ratio results.

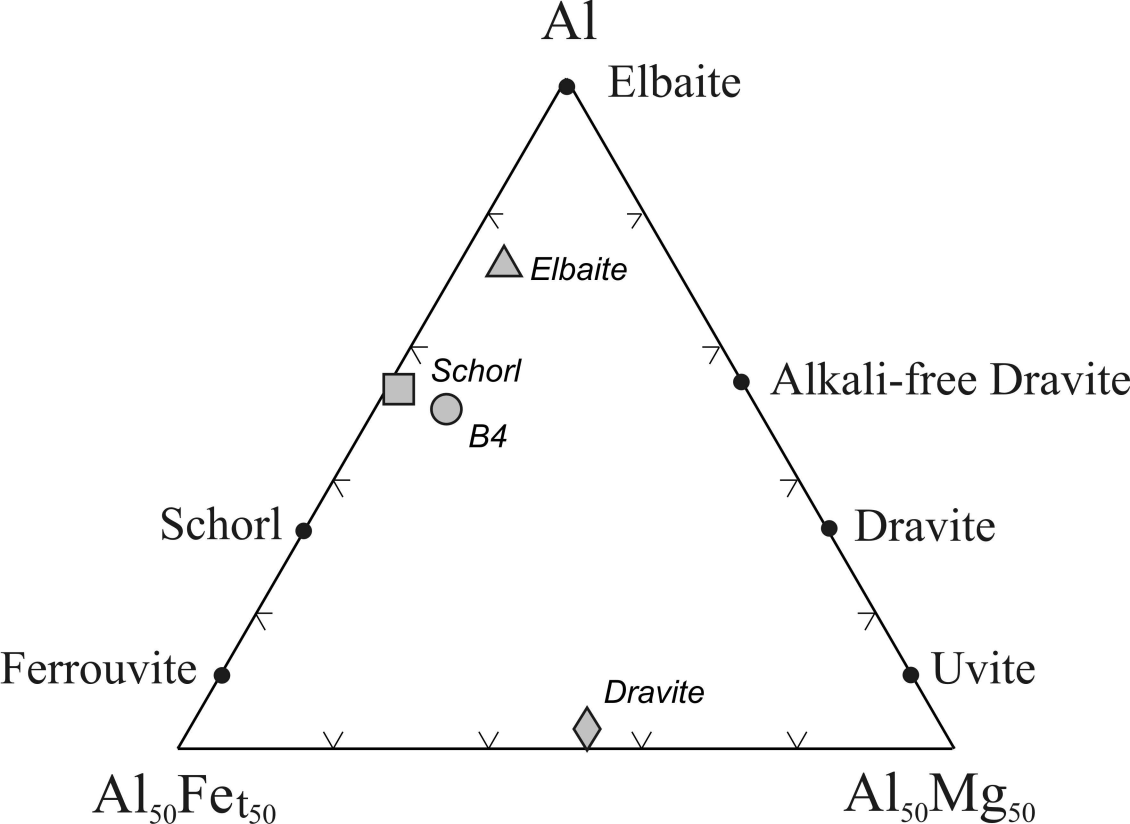


Table 1. Summary results of electron microprobe homogeneity tests.

SCHORL 112566.1		SiO ₂	TiO ₂	Al_2O_3	FeO	MnO	MgO	CaO	Na ₂ O	K ₂ O	B_2O_3
	Potsdam										
Fragment 1	mean	32.20	0.66	32.01	14.87	1.05	0.19	0.16	2.12	0.05	10.04
	1s (n = 4)	0.29	0.05	0.13	0.32	0.22	0.03	0.03	0.08	0.02	0.44
Fragment 5	mean	32.34	0.51	32.20	14.72	1.06	0.23	0.17	2.10	0.03	10.10
	1s (n = 4)	0.25	0.02	0.11	0.50	0.07	0.03	0.02	0.07	0.03	0.49
Fragment 9	mean	32.50	0.65	31.85	14.15	1.03	0.18	0.16	2.06	0.04	10.17
	1s (n = 4)	0.31	0.06	0.35	0.76	0.09	0.02	0.03	0.07	0.03	0.28
Fragment 12	mean	32.51	0.49	32.08	14.60	1.07	0.22	0.14	2.12	0.04	10.37
	1s (n = 4)	0.59	0.07	0.18	0.50	0.18	0.03	0.03	0.06	0.03	0.22
Fragment 14	mean	32.48	0.68	31.61	14.99	0.88	0.26	0.13	2.12	0.05	10.01
	1s (n = 4)	0.56	0.07	0.17	0.38	0.07	0.02	0.05	0.05	0.02	0.26
Fragment 15	mean	32.28	0.66	32.01	14.13	1.18	0.18	0.13	2.16	0.06	10.04
Calcad annual access	1s (n = 4)	0.37	0.09	0.32	0.33	0.16	0.04	0.06	0.05	0.02	0.22
Schorl grand mean	100/- 24	32.37	0.63	31.99	14.55	1.02	0.21	0.15	2.13	0.04	10.11
	1SD (n = 24) 1SD (%)	0.44 1.37	0.10	0.30 0.95	0.60 4.15	0.17	0.04	0.04	0.07	0.03 59.97	0.37 3.62
	130 (%)	1.57	16.73	0.95	4.15	16.62	19.88	27.93	3.38	59.97	5.02
	Madison										
Fragment 1	mean	33.43	0.54	34.33	15.05	1.13	0.22	0.15	2.01	0.03	9.23
ruginent 1	1s (n = 4)	0.06	0.02	0.13	0.08	0.06	0.01	0.01	0.07	0.01	0.64
Fragment 2	mean	33.23	0.54	34.42	14.63	1.23	0.21	0.14	2.03	0.05	9.30
	1s (n = 4)	0.15	0.02	0.11	0.15	0.06	0.01	0.01	0.06	0.01	0.42
Fragment 3	mean	33.35	0.57	33.74	15.52	1.17	0.29	0.17	2.06	0.04	10.01
· ·	1s (n = 4)	0.22	0.06	1.52	1.59	0.22	0.19	0.05	0.16	0.01	0.43
Fragment 4	mean	33.42	0.52	34.19	14.85	1.19	0.19	0.13	2.02	0.04	9.77
	1s (n = 4)	0.14	0.02	0.16	0.13	0.08	0.02	0.02	0.04	0.00	0.46
Fragment 5	mean	32.84	0.57	34.29	14.57	1.22	0.20	0.13	1.97	0.04	10.17
	1s (n = 4)	0.16	0.02	0.05	0.12	0.04	0.01	0.01	0.06	0.01	0.81
Fragment 6	mean	33.37	0.55	34.39	14.73	1.20	0.18	0.13	2.05	0.04	9.34
	1s (n = 4)	0.16	0.01	0.10	0.13	0.04	0.02	0.01	0.04	0.01	0.72
Schorl grand mean		33.3	0.55	34.2	14.9	1.19	0.21	0.14	2.02	0.04	9.64
	1s (n = 24)	0.25	0.03	0.60	0.67	0.10	0.08	0.03	0.08	0.01	0.65
	1s (%)	0.75	5.71	1.77	4.50	8.40	37.25	17.80	3.99	22.49	6.74
Dyar et al. (2001)	mean	33.4	0.57	33.1	17.3	1.20	0.21	0.11	1.92	0.02	*11.4
DRAVITE 108796.1											
DRAVIIL 1007 30.1	Potsdam										
Fragment 1	mean	33.05	1.58	20.88	15.63	0.08	7.86	2.41	1.60	0.10	9.60
	1s (n=4)	0.31	0.06	0.18	0.39	0.10	0.08	0.11	0.04	0.03	0.32
Fragment 2	mean	33.39	1.52	22.38	13.76	0.03	8.28	2.30	1.71	0.06	10.44
· ·	1s (n=4)	0.28	0.08	0.22	0.62	0.05	0.15	0.09	0.04	0.04	0.45
Fragment 3	mean	33.20	1.49	22.31	13.91	0.02	8.11	2.39	1.74	0.06	10.21
	1s (n=4)	0.29	0.17	0.20	0.13	0.04	0.13	0.08	0.07	0.04	0.26
Fragment 4	mean	33.30	1.53	21.33	15.31	0.00	8.14	2.59	1.47	0.06	9.93
	1s (n=4)	0.07	0.10	0.21	0.79	0.00	0.11	0.06	0.08	0.01	0.39
Fragment 5	mean	32.81	1.53	20.87	15.47	0.05	8.16	2.67	1.43	0.05	10.57
	1s (n=4)	0.33	0.08	0.28	0.63	0.05	0.20	0.08	0.05	0.02	0.34
Fragment 6	mean	33.24	1.49	22.09	14.78	0.08	8.25	2.29	1.76	0.10	10.13
	1s (n=4)	0.19	0.11	0.17	0.41	0.09	0.08	0.09	0.03	0.02	0.28
Dravite grand mean		33.16	1.52	21.64	14.81	0.05	8.13	2.44	1.62	0.07	10.15
	1s (n=24)	0.33	0.11	0.69	0.93	0.07	0.20	0.17	0.14	0.03	0.48
	1s (%)	0.99	7.47	3.19	6.30	161.86	2.40	6.92	8.89	50.00	4.74
DRAVITE 108796.1											
DRAVIIL 1007 30.1	Madison										
Fragment 1	mean	34.10	1.60	23.40	13.89	0.01	8.92	2.32	1.69	0.06	10.37
	1s (n = 4)	0.14	0.02	0.10	0.25	0.01	0.04	0.02	0.03	0.01	0.74
Fragment 2	mean	33.79	1.86	21.87	16.24	-0.02	8.30	2.72	1.50	0.06	10.00
-	1s (n = 4)	0.23	0.02	0.07	0.14	0.01	0.09	0.02	0.03	0.01	0.24
Fragment 3	mean	34.29	1.59	23.36	13.86	0.03	8.93	2.32	1.72	0.06	9.88
-	1s (n = 4)	0.15	0.04	0.19	0.24	0.01	0.12	0.02	0.07	0.01	0.22
Fragment 4	mean	34.50	1.72	23.41	14.28	0.00	8.48	2.46	1.64	0.07	10.18
5											

Table 2. Summary of SIMS homogeneity tests for lithium concentration and new working value.

					Li ₂ C) (m/10	0m)
		7Li ⁺ /28Si ⁺	precision ^b	this study ^c	Dyar 1	Dyar 2	Dyar 3
SCHORL 112566.1	mean	0.1403	0.81%	0.1176	0.09	0.107	0.071
	1s (n = 30)	0.0105		0.0087			
	repeat. (1s, %) ^a	7.4		7.4			
DRAVITE 108796.1	l mean	0.00207	1.94%	0.00177	nr	0.017	0.00095
	1s (n = 28)	0.00028		0.00024			
	repeat. (1s, %) ^a	13.6		13.6			
ELBAITE 98144.1	mean	2.12	0.27%	1.92	1.33	0.98	0.30
	1s (n = 36)	0.21		0.19			
	repeat. (1s, %) ^a	9.8		9.8			
NIST 610	mean	0.0567	0.68%				
	1s (n = 19)	0.0015					
	repeat. (1s, %) ^a	2.6					

nr = not reported

a. repeatability from "n" repeat measurements as 1s (mean value in percent). See supplemental tab b. mean internal precision from 20 cycles per measurement (1s).

c. Li concentrations calibrated from NIST 610 glass, recommended SiO_2 value 69.4 m/100m and Li 46

d. Li concentrations reported by Dyar et al. (2001) based on (1) PIGE, (2) flame AAS, (3) SIMS, (4) ICF

Dyar 4
nr
-
0.001
nr

le 2 for information about the distribtion of SIMS results.

 $58~\mu g/g$ (Jochum et al. 2011). SiO_2 values for tourmalines used in calculation is mean of 3 -AES.



Table 3. Summary of SIMS homogeneity tests for lithium isotope ratio.

		⁷ Li / ⁶ Li	cycles	int. precision ^b	beam current	⁷ Li cps
SCHORL 112566.1	mean	11.6316	50	0.17 ‰	3.5 nA	3.9E+06
	1s (n = 44)	0.0087				
	repeatability ^a	0.75 ‰				
DRAVITE 108796.1	mean	12.16830	150	0.3 ‰	12 nA	1.9E+05
	1s (n = 36)	0.02630				
	repeatability ^a	2.16 ‰				
ELBAITE 98144.1	mean	12.71700	25	0.08 ‰	4.5 nA	7.6E+07
	1s (n = 38)	0.00430				
	repeatability ^a	0.33 ‰				
NIST 610	mean	11.81660	50	0.08 ‰	3.5 nA	2.6E+06
	1s (n = 8)	0.00500				
	repeatability ^a	0.43 ‰				

n = number of determinations, this also includes the data from the small "DM" area nd = not determined

Values for beam current, ⁷Li count rate and internal precision are average of "n" measurements. All data are reported in Electronic Supplement Table 3.

- a. repeatability from "n" repeat measurements as 1s (in %).
- b. internal precision from "n" cycles as 1 sd / mean in permil
- c. ion detection method EM = electron multiplier, FC = Faraday cup
- d. Amount of material sputtered based on white light profilometry and an assumed density of $\rho = 3$

detector ^c	test mass (ng)
EM/FC	0.10
EM/EM	1.3
FC/FC	~0.07
EM/FC	nd

3.0 g/cm³

Table 4. Summary of SIMS homogeneity tests for oxygen isotope ratio.

		¹⁸ O / ¹⁶ O (meas.)	¹⁸ O / ¹⁶ O (corr.) ^b	int. precision ^c
SCHORL 112566.1	CHORL 112566.1 mean		0.00201709	0.11‰
	1s (n = 63)	5.47E-07	5.39E-07	
	repeatability ^a	0.27‰	0.27‰	
DRAVITE 108796.1	mean	0.00202194	0.00202103	0.10‰
	1s (n = 47)	5.12E-07	4.42E-07	
	repeatability ^a	0.25‰	0.22‰	
ELBAITE 98144.1	mean	0.00202725	0.00202645	0.11‰
	1s (n = 70)	6.12E-07	4.55E-07	
	repeatability ^a	0.30‰	0.22‰	
NIST 610	mean	0.00203007	0.00202942	0.10‰
	1s (n = 29)	6.68E-07	4.28E-07	
	repeatability ^a	0.33‰	0.21‰	
All 1 .	repeatability	0.55%	U.Z1700	

All data are reported in Electronic Supplement Table 4.

a. repeatability from "n" measurements (1s).

b. corrected for linear drift based on NIST 610 results, see text.

c. mean internal precision from "n" cycles (1s).

d. $^{18}\text{O}/^{16}\text{O}$ instrumental mass fractionation (measured ratio / true), based on the grand mean

e. uncertainty in % of the recomended δ value of this material (see table 7).

lMF ^d	IMF uncet. ^e
0.99630	0.030
0.99785	0.1
0.00035	0.0
0.99825	0.0
1.0	

 δ^{18} O values indicated on table 6.

Table 5. Summary results of $\delta^7 \text{Li}_{\text{L-SVEC}}$ by solution ICP mass spectrometry, values in ‰.

Material	Laboratory	dissolution	No of analyses	δ ⁷ Li (mean) ‰	δ^7 Li (range) ‰
SCHORL 112566.1	Bremen	1	5	5.71	5.52 - 5.88
	Maryland	1	2	4.24	4.22 - 4.26
	Maryland	2	2	4.81	4.64 - 4.98
	Bristol	1	2	5.64	5.60 - 5.72
	Bristol	2	2	5.71	5.64 - 5.78
	Woods Hole	1	4	5.52	5.35 - 5.70
	Woods Hole	2	4	5.29	4.70 - 5.66
	Median ^a			5.52 ± 0.23	
DRAVITE 108796.	1 Bremen	1	2	10.99	nd
	Maryland	1	2	8.72	7.97 - 9.35
	Maryland	2	1	8.78	8.21 - 9.34
	Bristol	1	3	10.17	10.10 - 10.25
	Bristol	2	2	10.24	10.14 - 10.35
	Woods Hole	1	1	9.67	nd
	Woods Hole	2	1	10.24	nd
	Median			10.17 ± 0.34	
ELBAITE 98144.1	Bremen	1	5	7.10	6.94 -7.28
	Maryland	1	2	6.04	5.84 - 6.24
	Maryland	2	2	6.87	6.64 - 7.11
	Bristol	1	3	7.18	7.12 - 7.24
	Bristol	2	2	7.71	7.62 - 7.81
	Woods Hole	1	4	7.13	6.80 - 7.34
	Median ^a			7.12 ± 0.24	

See electronic supplement 5 for a complete report of all individual results.

nd = not defined, 1s repeatability values only reported for those aliquots with \geq 3 mass spectrometer determin a. Median of n = 6 or 7 independent dissolutions with 1SE based on the 1s reproducibility divided by b Values in % reported by Lin et al. (2019) for comparison based on n = 3 determinations using mircodrilling ϵ

Lin et al. (2019) ^b
6.47 ± 0.20
7.90 ± 0.22

ations.

sqrt(n-1).

and wet chemical methods, uncertainty estimates are 1s.

Table 6. Summary results of oxygen isotope ratio analyses by gas source mass spectrometr

				$\delta^{18} O_{SMOW}$	
Material	Laboratory	session	n ^b	mean	range ^c
SCHORL 112566.1	Cape Town	1	2	9.59	9.54 - 9.64
	Cape Town	2	2	9.75	9.66 - 9.83
	Milton Keynes	1	2	9.71	9.68 - 9.74
	Milton Keynes	2	2	9.71	9.71 - 9.71
	Madison	1	2	9.76	9.74 - 9.77
	Madison	2	2	9.63	9.58 - 9.67
	Keyworth	1	2	9.49	9.74 - 9.61
	Keyworth	2	2	9.65	9.33 - 9.97
	Keyworth	3	1	9.46	
	E. Kilbride	1	3	9.70	9.59 - 9.78
	Göttingen	1	1	9.81	
	Göttingen	2	2	9.70	9.47 - 9.81
(aaaa)	Grand Mean ^a			9.66 ± 0.03	
Dyar et al. (2001)				10.32 ± 0.03	
DRAVITE 108796.1	Cape Town	1	2	9.99	9.98 - 9.99
	Cape Town	2	2	10.01	9.90 - 10.12
	Milton Keynes	1	1	10.04	10.00 10.10
	Milton Keynes	2	2	10.07	10.02 - 10.12
	Madison	1	2	10.19	10.17 - 10.20
	Madison	2	2	10.01	9.99 - 10.02
	Keyworth	1	2	9.75	9.50 - 10.0
	Keyworth	2	2	10.62	10.59 - 10.74
	E. Kilbride	1	4	9.92	9.80 - 9.99
	Göttingen	1	3	10.13	10.12 - 10.16
Dyar et al. (2001)	Grand Mean ^a			10.07 ± 0.08 10.03 ± 0.02	
ELBAITE 98144.1	Cape Town	1	2	13.71	13.69 - 13.73
	Cape Town	2	2	13.74	13.71 - 13.77
	Milton Keynes	1	2	13.81	13.77 - 13.85
	Milton Keynes	2	2	13.87	13.87 - 13.87
	Madison	1	3	13.87	13.81 - 13.92
	Madison	2	2	13.96	13.84 - 14.08
	Keyworth	1	1	14.52	
	Keyworth	2	1	12.72	
	Keyworth	3	1	13.73	
	E. Kilbride	1	4	13.54	13.20 - 13.79
	Göttingen	1	3	13.94	13.82 - 14.00
	Grand Mean ^a			13.76 ± 0.13	
Dyar et al. (2001)				13.89 ± 0.02	
UWG-2 grnt	Cape Town		4	5.76	5.69 - 5.87
	Milton Keynes		4	5.75	5.69 - 5.80
	Madison		4	5.80	5.75 - 5.91
	Keyworth		3	5.49	5.07 - 5.98
	E. Kilbride		9	5.75	5.63 - 5.87
	Göttingen		15	5.77	5.62 - 5.90

See electronic supplement 6 for a complete report of all individual results.

a. simple mean of n = 10, 11 or 12 independent sessions with 1SE based on the reproducibil

- b . number of independent determinations during the given analytical day. c. range only reported for those determinations containing ≥ 2 determinations.

$\delta^{17}O_{\text{SMOW}}$	
mean	range ^c
5.07	5.05 - 5.08
5.07	5.06 - 5.08
5.12	
5.06	4.93 - 5.12
5.08	
5.38 5.27	5.24 - 5.29
5.29 5.31	5.28 - 5.31
7.21 7.24	7.18 - 7.23 7.23 - 7.25
7.27 7.24	7.20 - 7.31
2.98	2.96 - 3.01
2.99	2.93 - 3.06

lity divided by sqrt(n-1).

Table 7. Compilation of reference values for the three Harvard troumaline materials.

	LiO ₂ Concentration	$\delta^7 \text{Li}_{\text{L-SVEC}}$	$\delta^{18}O_{SMOW}$
	(m/100m) ^a	(‰)	(‰)
Schorl 112566.1	0.118 ± 0.009	5.52 ± 0.23	9.66 ± 0.03
Dravite 108796.1	0.00177 ± 0.00024	10.17 ± 0.34	10.07 ± 0.08
Elbaite 98144.1	1.92 ± 0.19	7.12 ± 0.24	13.89 ± 0.02
Status	Current Best Estimate	Recommended Value	Recommended Value
uncertainty type	1s repeatability	1SE	1SE

a. Values based on SIMS data calibrated using silicat glass NIST 610 -- subject to uncontrolled ma

b. Values published by Dyar $\it et~\it al~.$ (2001) on starting materials.

c. Values published by Leeman and Tonarini (2001) on starting material.

d. Values published by Marger et al. (2020) on starting material.